

000 001 002 003 004 005 ROBUST TRAJECTORY DISTILLATION: HYBRID 006 REWEIGHTING MEETS TEACHER-INSPIRED TARGETS 007 008 009

010 **Anonymous authors**
011 Paper under double-blind review
012
013
014
015
016
017
018
019
020
021
022
023
024
025
026

ABSTRACT

027 Robust training under noisy labels remains a critical challenge in deep learning due
028 to the risk of confirmation bias and overfitting in iterative correction pipelines. In
029 this work, we propose a novel trajectory-based dataset distillation framework that
030 jointly addresses noise suppression and knowledge preservation without requiring
031 label correction or clean subsets. Our method introduces two complementary
032 components: Selective Guidance Reweighting (SGR) and Teacher-Inspired Aux-
033 iliary Targets (TIAT). SGR improves teacher signal quality by integrating global
034 forgetting patterns (via second-split forgetting) with local feature consistency (via
035 KNN-based evaluation), forming a hybrid reweighting mechanism that prioritizes
036 clean supervision. TIAT further enhances the learning capacity by injecting aux-
037 iliary guidance derived from intermediate teacher dynamics, ensuring internal
038 consistency while reinforcing informative signals. Together, these strategies enable
039 the distilled dataset to retain cleaner and richer knowledge representations under
040 noisy supervision. The proposed framework is label-preserving, computationally
041 efficient, and broadly applicable. Extensive experiments on benchmark datasets
042 demonstrate consistent performance improvements over state-of-the-art dataset
043 distillation methods across symmetric, asymmetric, and real-world noise scenarios.
044
045

1 INTRODUCTION

046 The growing complexity of deep learning models has heightened the dependence on large-scale, high-
047 quality datasets. However, real-world annotations are frequently affected by label noise, stemming
048 from factors such as human bias, inconsistencies in crowdsourced labeling, semantic ambiguities, and
049 errors in web-crawled pseudo-labels. Although manual relabeling could, in principle, address this
050 issue, it is often infeasible due to the substantial cost associated with correcting datasets containing
051 millions of samples (e.g. WebVision (Li et al., 2017)). As a result, developing robust learning
052 methods that can effectively handle noisy labels has emerged as a critical research challenge.
053

054 To mitigate the impact of noisy labels, a range of strategies has been proposed, including sample
055 selection (Malach & Shalev-Shwartz, 2017; Liu et al., 2020; Zhu et al., 2022), loss weighting (Zhang
056 & Sabuncu, 2018; Liu & Guo, 2020), and label correction (Reed et al., 2014; Song et al., 2019).
057 These approaches typically aim to estimate the likelihood of label corruption and adapt the training
058 process accordingly, either by down-weighting or excluding potentially noisy samples, or by explic-
059 itely correcting their labels. While such online, iterative optimization schemes have demonstrated
060 effectiveness in controlled experimental settings, the lack of reliable ground-truth validation anchors
061 (e.g., a clean subset) complicates the stabilization of the optimization trajectory, increasing the risk of
062 overfitting to unvalidated pseudo-labels and triggering self-reinforcing cycles of error amplification.
063

064 The limitations of conventional noisy label learning methods primarily arise from the tight coupling
065 between noise estimation and model training. At the core of these approaches is a self-referential
066 dilemma: the model simultaneously serves as both noise detector and target predictor, creating a
067 closed-loop system prone to confirmation bias amplification. This feedback loop often results in
068 overconfidence in incorrect labels, ultimately degrading generalization performance. Furthermore,
069 such methods typically depend on stable external anchors (e.g., verified clean subsets or other
070 prior knowledge) and resource-intensive iterative procedures, which increase computational costs
071 and deployment complexity. In real-world applications, these constraints significantly impede
072 scalability. Additionally, dynamic relabeling introduces security risks, as adaptive data modifications
073

054 unintentionally expose privacy-sensitive information. Recent advances (Cheng et al., 2024) suggest
 055 dataset distillation as a promising alternative: by synthesizing compact training subsets that preserve
 056 essential information, it enhances robustness under noisy supervision.

057 Although previous work (Cheng et al., 2024) has demonstrated the potential of dataset distillation in
 058 mitigating label noise, significant limitations remain regarding the efficiency and capacity of noise-to-
 059 clean knowledge transfer. Conventional distillation frameworks (Wang et al., 2018b; Cui et al., 2022)
 060 suffer from two key shortcomings: **(1) Noise-Agnostic Information Extraction:** Methods such as
 061 DANCE (Zhang et al., 2024a) and DATM (Guo et al., 2024) generally assume clean supervision and
 062 lack explicit mechanisms to suppress feature associations induced by corrupted labels. Consequently,
 063 their performance degrades under noise. For example, in symmetric noise with 20% noise rate on
 064 the CIFAR-10 dataset, both DATM and DANCE exhibit an accuracy drop of approximately 2% to
 065 3% compared to their performance in clean environments when the images per class (IPC) is 50.
 066 **(2) Capacity-Constrained Synthesis:** Synthetic datasets are typically parameterized as fixed-size
 067 image tensors (e.g., 50 IPC), which imposes a strict upper bound on their capacity to represent
 068 informative content. This limitation increases the risk of premature information compression, poten-
 069 tially discarding useful clean signals before sufficient disentanglement from noisy patterns can occur.
 070 These limitations motivate a central question: *How can we improve both the quality and capacity of*
 071 *distilled data under noisy supervision?* This challenge can be broken down into two complementary
 072 objectives:

073 **Challenge ①:** Improving the fidelity of the synthetic dataset by promoting cleaner knowledge
 074 retention and enhancing robustness to label noise through better teacher signal quality.

075 **Challenge ②:** Complementing intrinsic knowledge quality improvements by enhancing the effective-
 076 ness of knowledge transmission from teacher to student trajectories, allowing the synthetic dataset to
 077 absorb richer and cleaner supervision even under noise.

078 To this end, we propose two complementary techniques: **Selective Guidance Reweighting (SGR)**
 079 and **Teacher-Inspired Auxiliary Targets (TIAT)**, respectively. SGR enhances synthetic data learning
 080 by improving teacher trajectory quality. It integrates global forgetting trends via second-split
 081 forgetting (Maini et al., 2022; Li et al., 2022) with local neighborhood consistency through KNN-
 082 based evaluation, forming a hybrid reweighting scheme. This dynamic calibration ensures that the
 083 teacher’s guidance focuses more on clean supervision, thereby improving the overall teaching quality
 084 and enabling the student to learn more effectively. The underlying assumption is straightforward:
 085 a more reliable teacher produces a more capable student. TIAT are designed to further augment
 086 the distillation process by providing additional high-quality supervision signals beyond the primary
 087 teacher trajectory. Specifically, TIAT derives a set of auxiliary targets—akin to residual teaching
 088 signals—from the teacher’s own training dynamics, such as intermediate predictions or consistency-
 089 based feedback. These auxiliary targets act as complementary assignments that reinforce the primary
 090 supervision, helping the student model to consolidate and generalize the distilled knowledge more
 091 effectively. Importantly, although these signals are decoupled from the trajectory itself, they are
 092 grounded in the teacher’s behavior and thus maintain internal consistency within the distillation
 093 framework. By injecting such coherent, yet enriched guidance, TIAT enables the synthetic dataset to
 094 absorb more informative supervision without introducing conflicting objectives.

095 In summary, we propose a distillation framework specifically tailored for learning under noisy
 096 supervision. Conceptually, the framework resembles a teacher who not only refines their expertise
 097 to provide higher-quality instruction but also assigns “homework-like” auxiliary tasks that further
 098 reinforce and consolidate the student’s learning outcomes. Our contributions are as follows:

- 101 • We introduce a progressive mechanism that integrates both dynamic and static sample
 102 reweighting, enabling the fusion of diverse teacher trajectory signals to achieve robust and
 103 superior noise suppression.
- 104 • We propose an auxiliary guidance regularization strategy that ensures clean trajectory
 105 consistency during distillation, effectively strengthening the influence of clean samples
 106 throughout the process.
- 107 • Our framework is label-preserving and computationally efficient, requiring no relabeling or
 108 extensive retraining, making it practical for real-world noisy data scenarios.

108 • Extensive experiments demonstrate that our framework consistently improves distillation
 109 performance across diverse datasets and noise settings, validating its generality and robust-
 110 ness.

111
 112 **2 RELATED WORKS**
 113

114 **2.1 LEARNING WITH NOISY LABELS**
 115

116 Real-world datasets often contain corrupted labels due to annotation errors or automated collection.
 117 To address this, noisy label learning has developed three major strategies: *sample selection*, *label*
 118 *correction*, and *sample reweighting*. Sample selection methods aim to identify clean data during
 119 training, typically using loss-based filtering. A representative work is Decoupling (Malah & Shalev-
 120 Shwartz, 2017), which introduced the small-loss trick. Follow-up works (Jiang et al., 2018; Han
 121 et al., 2018) incorporate external guidance or co-training, while curriculum-based methods (Lyu &
 122 Tsang, 2019; Zhou et al., 2021) and early-learning regularization (Liu et al., 2020) enhance robustness
 123 via dynamic filtering or temporal consistency. Some approaches even detect noisy samples prior to
 124 training (Zhu et al., 2022; Wang et al., 2018a). Label correction methods refine labels using model
 125 predictions (Reed et al., 2014; Zhou et al., 2024), semi-supervised strategies (Li et al., 2020), or
 126 meta-learning and neighborhood consistency (Tu et al., 2023; Li et al., 2022). Sample reweighting
 127 strategies (Zhang & Sabuncu, 2018; Shu et al., 2019; Di Salvo et al., 2024) instead adjust loss
 128 contributions based on sample reliability. Additionally, K-NN-based methods (Bahri et al., 2020;
 129 Iscen et al., 2022) have proven effective for noise detection by evaluating local label consistency in
 130 the feature space. Building on this, dataset distillation has recently emerged as a promising alternative.
 131 As shown in (Cheng et al., 2024), it addresses limitations such as iterative error amplification and
 132 privacy concerns, while offering strong performance under noisy supervision.

133 **2.2 DATASET DISTILLATION**
 134

135 Dataset distillation (Sachdeva & McAuley, 2023; Wang et al., 2018b; Cui et al., 2022) aims to
 136 compress a large dataset into a compact synthetic set while preserving downstream performance.
 137 The foundational work (Wang et al., 2018b) introduced the idea of optimizing synthetic data to
 138 match training dynamics observed on real data. Subsequent research has evolved along three
 139 major paradigms: *meta-learning*, *parameter matching*, and *distribution matching*. Meta-learning
 140 methods (Nguyen et al., 2021; Zhou et al., 2022; Loo et al., 2023) adopt a bi-level optimization
 141 framework to generalize across model initializations but suffer from high computational overhead.
 142 Parameter matching, including gradient (Zhao et al., 2021) and trajectory matching (Cazenavette
 143 et al., 2022; Du et al., 2023), directly aligns model updates between real and synthetic data, with
 144 trajectory-based methods achieving state-of-the-art results (Guo et al., 2024). Variants further explore
 145 progressive optimization (Chen et al., 2023), hybrid data composition (Lee & Chung, 2024), and
 146 group-wise structures (He et al., 2024). Distribution matching offers an efficient alternative by aligning
 147 real and synthetic data distributions in feature space (Zhao & Bilen, 2022; Zhang et al., 2024b), class
 148 relations (Deng et al., 2024), or image-label correlations (Zhang et al., 2024a), without requiring
 149 nested optimization. Recent advances even reformulate this as neural feature alignment (Wang et al.,
 150 2025). However, most methods assume clean supervision and degrade under real-world label noise.
 151 To address this limitation, we propose a noise-aware extension of trajectory matching that explicitly
 152 models and suppresses corruption during both the distillation and deployment phases.

153 **3 PRELIMINARIES**
 154

155 **3.1 NOISY DATASET DISTILLATION**
 156

157 Let $\mathcal{D}_{\text{real}} = \{(x_i, \tilde{y}_i)\}_{i=1}^N$ denote a real-world training dataset, where \tilde{y}_i is the observed (and poten-
 158 tially noisy) label for input x_i . We assume the existence of label noise such that $\tilde{y}_i \neq y_i^*$ for some i ,
 159 where y_i^* is the clean but unobserved ground-truth label. In contrast, the test set $\mathcal{D}_{\text{test}}$ is assumed to be
 160 entirely clean and representative of the true data distribution, and is used to evaluate generalization
 161 performance. Our objective is to synthesize a compact dataset \mathcal{S} , with $|\mathcal{S}| \ll |\mathcal{D}_{\text{real}}|$, such that a
 162 model trained solely on \mathcal{S} achieves lower generalization error on $\mathcal{D}_{\text{test}}$ than one trained on the full

162 noisy dataset $\mathcal{D}_{\text{real}}$. Formally, the distillation task can be formulated as the following optimization
 163 problem:

$$164 \quad \mathcal{S}^* = \arg \min_{\mathcal{S}} \mathcal{L}(\mathcal{S}, \mathcal{D}_{\text{real}}), \quad (1)$$

166 where \mathcal{L} is a general objective function. In our setting, it is instantiated as a trajectory matching
 167 loss (Guo et al., 2024) that aligns the student’s learning dynamics (trained on \mathcal{S}) with those of a
 168 teacher model trained on $\mathcal{D}_{\text{real}}$.

169 Trajectory matching-based dataset distillation methods typically adopt a bilevel optimization scheme
 170 comprising an *inner loop* and an *outer loop*. The inner loop simulates the training dynamics of
 171 a student model on the current synthetic dataset \mathcal{S} , while the outer loop updates \mathcal{S} such that the
 172 student’s optimization trajectory closely matches that of a teacher trained on the real dataset $\mathcal{D}_{\text{real}}$.

173 Specifically, a teacher model is first trained on $\mathcal{D}_{\text{real}}$ to produce a reference trajectory $\tau^* = \{\theta_t^*\}_{t=1}^T$,
 174 where θ_t^* denotes the model parameters at iteration t . Meanwhile, the synthetic dataset \mathcal{S} is initialized—either by sampling from Gaussian noise or selecting real samples—with corresponding soft or
 175 hard labels.

177 In the *inner loop*, we simulate student learning dynamics by iteratively updating parameters using \mathcal{S} .
 178 Given a starting point $\hat{\theta}_t = \theta_t^*$, the student parameters are updated over N steps according to:

$$180 \quad \hat{\theta}_{t+n+1} = \hat{\theta}_{t+n} - \alpha \nabla_{\hat{\theta}_{t+n}} \ell(\mathcal{A}(\mathcal{S}); \hat{\theta}_{t+n}), \quad (2)$$

182 where ℓ denotes the task loss (e.g., cross-entropy), $\mathcal{A}(\mathcal{S})$ denotes a mini-batch drawn from \mathcal{S}
 183 with optional data augmentation, and α is the learning rate. This simulates the student trajectory
 184 $\hat{\tau} = \{\hat{\theta}_{t+n}\}_{n=1}^N$ induced by \mathcal{S} .

185 In the *outer loop*, we optimize the synthetic dataset \mathcal{S} such that the student’s final parameters align
 186 with the teacher’s future trajectory. Let $\mathcal{T} = \{t_1, t_2, \dots, t_K\}$ be a set of anchor steps. At each $t \in \mathcal{T}$,
 187 the teacher parameters after M additional steps are denoted as θ_{t+M}^* . In our method, \mathcal{L} in Eq. 1 is
 188 instantiated as the following normalized trajectory alignment loss:

$$190 \quad \mathcal{L}_{\text{traj}}(\mathcal{S}, \mathcal{D}_{\text{real}}) = \frac{\|\hat{\theta}_{t+N} - \theta_{t+M}^*\|_2^2}{\|\theta_t^* - \theta_{t+M}^*\|_2^2}. \quad (3)$$

194 The normalization term $\|\theta_t^* - \theta_{t+M}^*\|_2^2$ calibrates the alignment error relative to the teacher’s own
 195 parameter change, making the loss scale-invariant across steps. The numerator measures how closely
 196 the student, trained on \mathcal{S} , approximates the teacher’s future parameters, while the denominator
 197 normalizes for the teacher’s update magnitude to ensure scale invariance. This outer-loop objective
 198 is used to update \mathcal{S} via gradient-based optimization, enabling the synthetic data to induce faithful
 199 learning dynamics that reflect those observed on real data.

200 4 METHODOLOGY

201 4.1 OVERVIEW

205 Figure 1 illustrates the overall workflow of our proposed framework for noisy dataset distillation,
 206 which aims to construct a compact synthetic dataset \mathcal{S} from a noisy real-world dataset $\mathcal{D}_{\text{real}} = (x_i, \tilde{y}_i)$.
 207 The core idea is to enable the student model trained on \mathcal{S} to replicate the learning dynamics of a
 208 teacher model trained on $\mathcal{D}_{\text{real}}$, while suppressing the adverse effects of label noise. To this end, our
 209 framework follows a three-stage pipeline. First, we train a teacher model on $\mathcal{D}_{\text{real}}$ to obtain a reference
 210 parameter trajectory $\tau^* = \theta_t^*$; during this stage, we apply *Selective Guidance Reweighting (SGR)*
 211 (See Sec. 4.2) to assign sample-specific weights based on reliability estimates derived from second-
 212 split forgetting and KNN-based local consistency, thereby producing a cleaner supervision signal.
 213 Second, we initialize a synthetic dataset \mathcal{S} with soft or hard labels and simulate the inner-loop training
 214 dynamics of a student model on \mathcal{S} . In this stage, we further incorporate *Teacher-Inspired Auxiliary*
 215 *Targets (TIAT)* (See Sec. 4.3)—a set of auxiliary consistency signals extracted from intermediate
 Finally, in the outer loop, we optimize \mathcal{S} via a normalized trajectory matching loss computed across

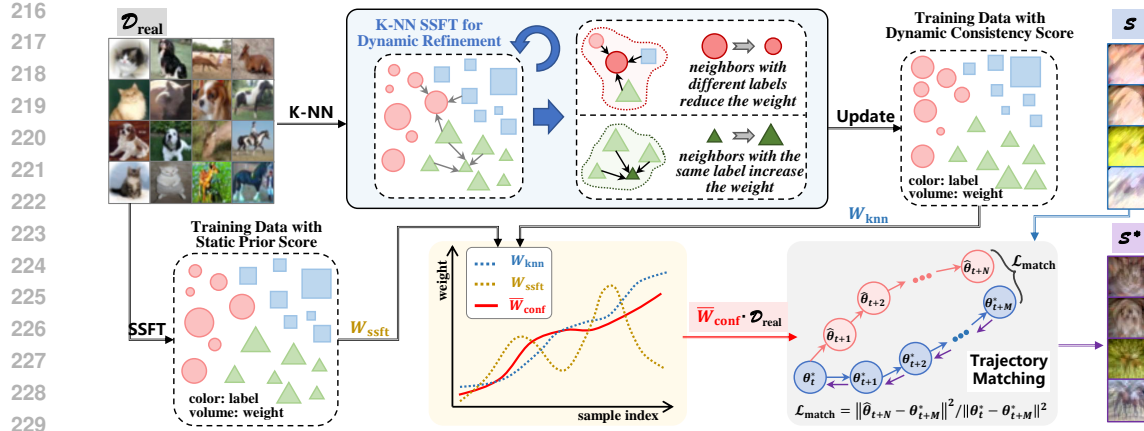


Figure 1: **The overall pipeline.** Our proposed pipeline includes two main contributions: (1) during teacher trajectory training, we apply sample-specific weighting adjustments to modulate the influence of each sample based on its estimated reliability; and (2) in the subsequent distillation phase, we utilize a subset of high-confidence samples to impose additional constraints and regularization, thereby enhancing the quality and generalization of the distilled dataset.

multiple anchor steps, aligning the student’s learned trajectory with that of the teacher. This bilevel optimization process jointly improves the quality of supervision (via SGR) and the effectiveness of trajectory alignment (via TIAT), enabling the distilled dataset to retain cleaner, more generalizable knowledge even under noisy conditions.

4.2 SELECTIVE GUIDANCE REWEIGHTING

We propose **Selective Guidance Reweighting (SGR)** to control the fidelity of signals used for synthetic data optimization. SGR introduces a hybrid reliability estimator for each training sample i , composed of:

- a **dynamic consistency score** $W_{\text{knn}}^{(i)}$ based on feature-space neighborhood agreement.
- a **static prior score** $W_{\text{ssft}}^{(i)}$ derived from sample forgetting behavior;

These scores are combined into a unified weight $W^{(i)}$ via time-dependent convex interpolation.

Dynamic Estimation via KNN. Given the predicted label distributions \hat{y}_j of the K nearest neighbors of the observed sample i in the feature space, we define its KNN consistency score as:

$$W_{\text{knn}}^{(i)} = 1 - \frac{1}{K} \sum_{j=1}^K \text{JS}(\bar{y}_i, \hat{y}_j), \quad (4)$$

where $\text{JS}(\cdot, \cdot)$ denotes Jensen-Shannon divergence. This score ranges in $[0, 1]$, with higher values indicating better local agreement.

Static Prior via SSFT. Inspired by (Maini et al., 2022), we introduce a forgetting-based difficulty score to quantify the reliability of each training sample. For each sample i , we record:

- $t_{\text{learn}}^{(i)}$: the earliest epoch when the sample is first correctly classified;
- $t_{\text{forget}}^{(i)}$: the earliest epoch after which it is misclassified again.

These timestamps reflect the memorization and retention behavior of a sample during training. To assess sample-level difficulty, we define the SSFT score as:

270

$$s^{(i)} = \lambda \cdot \frac{t_{\text{learn}}^{(i)}}{\max_j t_{\text{learn}}^{(j)}} + (1 - \lambda) \cdot \left(1 - \frac{t_{\text{forget}}^{(i)}}{\max_j t_{\text{forget}}^{(j)}}\right), \quad (5)$$

274 where $\lambda \in [0, 1]$ balances the contributions of learnability and forgettability. A high $s^{(i)}$ implies that
 275 sample i was learned late and forgotten early, thus more likely to be noisy or difficult. We convert
 276 this difficulty score into a static reliability weight:

$$W_{\text{ssft}}^{(i)} = 1 - s^{(i)}, \quad (6)$$

280 such that clean and stable samples are assigned higher weights at the beginning of training. This
 281 reflects the global memorization difficulty of sample i , with higher scores favoring clean samples
 282 with high probabilities.

283

284 **Hybrid Weighting via Curriculum Fusion.** To balance global priors and evolving local consis-
 285 tency, we define a convex combination:

$$W_t^{(i)} = (1 - \alpha_t) \cdot W_{\text{ssft}}^{(i)} + \alpha_t \cdot W_{\text{knn}}^{(i)}, \quad (7)$$

288 where $\alpha_t \in [0, 1]$ is a time-dependent blending coefficient that increases linearly over training epochs.
 289 Specifically, we set:

$$\alpha_t = \min \left(\frac{t}{T_{\text{warmup}}} \cdot \alpha_{\text{max}}, \alpha_{\text{max}} \right), \quad (8)$$

292 where T_{warmup} is a predefined transition period (e.g., 20% of training). Optionally, when training
 293 multiple teacher trajectories indexed by $p \in \{1, \dots, P\}$, we set $\alpha_{\text{max}}^{(p)} = \frac{p-1}{P}$ to diversify the
 294 static-dynamic balance across teachers (more details can be refer to Eq. 9).

295

296 **Remark.** The timestep weight $W_t^{(i)}$ is used to modulate the contribution of sample i when updating
 297 the teacher model parameters or computing guidance for \mathcal{S} in outer-loop optimization. This strategy
 298 enables the distillation process to prioritize clean, informative signals throughout training.

300

301 4.3 TEACHER-INSPIRED AUXILIARY TARGETS (TIAT)

302

303 While the **Selective Guidance Reweighting (SGR)** module focuses on suppressing noisy signals
 304 during teacher trajectory training, it does not explicitly constrain the distilled dataset \mathcal{S} to remain
 305 aligned with clean supervision. To address this limitation, we introduce **Teacher-Inspired Auxiliary**
 306 **Targets (TIAT)**, which injects clean-aware regularization into the distillation process by mining a
 307 reliable subset and incorporating trajectory-level uncertainty.

308

309 **Probabilistic Confidence Aggregation.** Let $W_p^{(i)}$ denote the final-stage reliability weight assigned
 310 to sample i by the p -th teacher trajectory, trained with static-dynamic blending coefficient $\alpha_{\text{max}}^{(p)}$. To
 311 estimate the sample's overall confidence, we define:

$$W_{\text{conf}}^{(i)} := \mathbb{E}_{p \sim \mathcal{U}(\mathcal{P})} \left[W_p^{(i)} \right] \approx \frac{1}{P} \sum_{p=1}^P W_p^{(i)}, \quad (9)$$

312

313 where $\mathcal{P} = \{1, \dots, P\}$ is the index set of all trajectories. This aggregated score summarizes the
 314 expected reliability of sample i across all teacher views.

315

316 We then compute the probabilistic trajectory alignment loss $\mathcal{L}_{\text{match}}$ that encourages student updates to
 317 follow the aggregated teacher behavior:

318

$$\mathcal{L}_{\text{match}} = \frac{1}{|\mathcal{S}|} \sum_{i \in \mathcal{S}} \frac{\|\hat{\theta}_{t+N}^{(i)} - \theta_{t+M}^*\|_2^2}{\|\theta_{t+M}^* - \theta_t^*\|_2^2}, \quad (10)$$

320

321 where $\hat{\theta}_{t+N}^{(i)}$ denotes the student parameters after training on synthetic sample i .

322

323

324 **Uncertainty-Aware Auxiliary Regularization.** To quantify confidence variance across trajectories,
 325 we compute:

$$327 \quad \text{Var}_p(W_p^{(i)}) = \mathbb{E}_{p \sim \mathcal{U}(\mathcal{P})} \left[\left(W_p^{(i)} - \bar{W}_{\text{conf}}^{(i)} \right)^2 \right]. \quad (11)$$

329 This variance reflects the stability of confidence scores assigned to sample i ; low-variance samples
 330 are deemed more consistently reliable.

331 We then define an approximately reliable subset \mathcal{D}_{sub} using two complementary criteria: $W_{\text{ssft}}^{(i)} \geq \delta_{\text{sup}}$
 332 and $\text{Var}_p(W_p^{(i)}) \leq \sigma_{\text{inf}}$, where δ_{sup} and σ_{inf} are fixed thresholds. This set captures samples that are
 333 both statistically confident and dynamically stable, forming the basis of our auxiliary regularization.
 334 Based on \mathcal{D}_{sub} , we fine-tune θ_t^* to produce a cleaner teacher checkpoint θ_{t+M}^{ft} and define the auxiliary
 335 loss as:

$$337 \quad \mathcal{L}_{\text{aux}} = \frac{1}{|\mathcal{S}|} \sum_{i \in \mathcal{S}} \frac{\|\hat{\theta}_{t+N}^{(i)} - \theta_{t+M}^{\text{ft}}\|_2^2}{\|\theta_{t+M}^{\text{ft}} - \theta_t^*\|_2^2}. \quad (12)$$

340 We integrate the original and fine-tuned guidance using a convex combination:

$$341 \quad \mathcal{L}_{\text{total}} = (1 - \beta) \cdot \mathcal{L}_{\text{match}} + \beta \cdot \mathcal{L}_{\text{aux}}, \quad \beta \in [0, 1], \quad (13)$$

343 where β balances the influence of the original and clean-adjusted trajectories.

345 **Discussion.** TIAT introduces an uncertainty-aware auxiliary supervision signal into dataset distilla-
 346 tion, driven by both trajectory consensus and variance-aware selection. By formulating confidence as
 347 a probabilistic mean and incorporating uncertainty, the method enables soft guidance that avoids hard
 348 filtering while remaining computationally efficient. This module complements SGR by enforcing
 349 trajectory-level regularization from the student side, forming a closed-loop distillation pipeline robust
 350 to noisy supervision.

352 5 EXPERIMENTS

354 5.1 EXPERIMENT SETUP

356 We evaluate our method on two widely used benchmarks in Noisy Label Learning (LNL) and Dataset
 357 Distillation (DD): CIFAR-10, CIFAR-100 (Krizhevsky, 2009). Comprehensive experiments are
 358 conducted under varying noise conditions and Image Per Class (IPC) configurations to assess the
 359 robustness and scalability of our approach.

360 **Noisy Settings** In alignment with previous work (Song et al., 2022; Englesson & Azizpour, 2024;
 361 Iscen et al., 2022), our evaluation includes both synthetic and real-world noise patterns:

- 363 • **Symmetric Noise:** Labels are uniformly corrupted across all non-target classes. Formally,
 364 given a noise rate η , a sample from class c has a probability η of being mislabeled as any
 365 class $c \neq c'$ with equal likelihood: $P(y_{\text{noisy}} = c' | y_{\text{clean}} = c) = \frac{\eta}{C-1}, \forall c' \neq c$, where C is
 366 the number of classes. We set $\eta \in \{20\%, 40\%\}$.
- 367 • **Asymmetric Noise:** Label flips follow class-dependent transition rules (e.g., cat \leftrightarrow dog,
 368 truck \rightarrow automobile).
- 369 • **Real-World Noise:** We adopt CIFAR-N Wei et al. (2021), a human-annotated variant of
 370 CIFAR-10/100 with natural labeling inconsistencies. Its multi-annotator design captures
 371 ambiguity patterns, providing a benchmark that aligns with real-world human cognition and
 372 a valid noise benchmark.

373 **Implementation** We compare our method against two baselines: (1) the noisy baseline, which
 374 involves training directly on the corrupted dataset, and (2) state-of-the-art distillation approaches,
 375 including DATM (Guo et al., 2024), DANCE (Zhang et al., 2024a), and RCIG (Loo et al., 2023). To
 376 ensure a fair comparison, we follow the key experimental settings in prior work, particularly DATM.
 377 Specifically, we use a three-layer ConvNet for CIFAR-10/100. For evaluation, we report the final
 378 mean and standard deviation of test accuracy by training 5 randomly initialized networks with \mathcal{S} .

378
379

5.2 BENCHMARKING DATASET DISTILLATION RESULTS ON NOISY DATASET

380
381
382
383
384
385
386
387
388
389
390
391
392
393
394

As shown in Figure 2, across all four noise scenarios, our method (red curves) has a higher accuracy than the three state-of-the-art baselines—RCIG (purple), DANCE (green), and DATM (blue). Across all settings, our method (red curves) consistently outperforms the baselines, particularly in high IPC regimes. The performance gap is most evident under higher noise (40%), where competing methods degrade rapidly, while our method maintains strong accuracy and smooth trends. Even under the challenging asymmetric noise setting, where existing dataset distillation methods typically suffer substantial performance drops, our approach consistently outperforms the baseline at both 20% and 40% noise levels. These results further confirm that our clean-aware sample reweighting and trajectory-informed distillation improve robustness against label corruption, especially when training data is both scarce and noisy. Table 1 compares our method with recent state-of-the-art approaches on **CIFAR-100N** and **CIFAR-100** under symmetric and asymmetric noise at 20% and 40% ratios. Across all IPC levels, our method achieves the best performance in nearly all settings. Notably, under 40% symmetric noise, we outperform prior methods by large margins—achieving **52.8%** at 100 IPC and **43.2%** at 10 IPC. Even in the challenging “**worse**” case, our method yields the highest result (**45.9%** at 50 IPC). These results highlight the robustness of our clean-aware reweighting and distillation design under severe label noise.

395
396
397

Table 1: Test accuracy (%) of our method and existing state-of-the-art methods on the **CIFAR-100N** and **CIFAR-100** with (a)symmetric noise ratios of 20% and 40%.

Noise Type Noise Ratio IPC	Symmetric						Asymmetric						worse	
	20%			40%			20%			40%			40.20%	
	10	50	100	10	50	100	10	50	100	10	50	100	10	50
Full Dataset	48.9±0.4			39.9±0.2			46.2±0.5			33.0±0.1			44.4±0.3	
RCIG (Loo et al., 2023)	41.2±0.3	38.4±0.3	-	36.5±0.4	30.7±0.2	-	38.9±0.4	37.5±0.2	-	28.7±0.4	27.9±0.3	-	37.0±0.3	35.3±0.2
DANCE (Zhang et al., 2024a)	45.8±0.2	48.0±0.3	47.5±0.2	39.7±0.2	42.0±0.4	42.6±0.3	43.8±0.3	46.7±0.3	48.2±0.4	32.2±0.4	34.2±0.2	35.22±0.3	42.0±0.3	43.6±0.3
DATM (Guo et al., 2024)	45.1±0.1	49.7±0.3	48.9±0.2	40.6±0.4	45.1±0.4	44.4±0.3	40.3±0.4	45.4±0.3	50.2±0.3	29.4±0.4	32.0±0.3	36.0±0.3	39.9±0.5	43.9±0.2
Ours	45.8±0.3	51.6±0.1	55.7±0.2	43.2±0.2	48.4±0.4	52.8±0.2	44.6±0.2	50.3±0.3	54.4±0.1	34.7±0.1	36.5±0.4	40.7±0.4	41.0±0.3	45.9±0.1

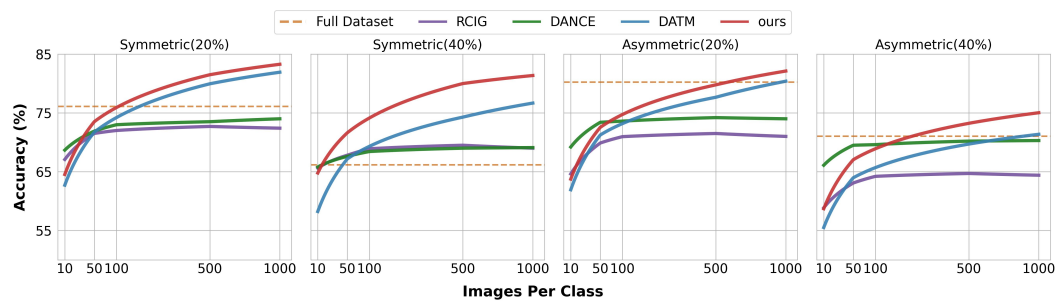
416
417

Figure 2: Test accuracy (%) of our method and existing state-of-the-art methods on the **CIFAR-10** with (a)symmetric noise ratios of 20% and 40%.

418
419

5.3 ABLATION STUDIES

420
421
422
423
424
425
426
427
428
429
430

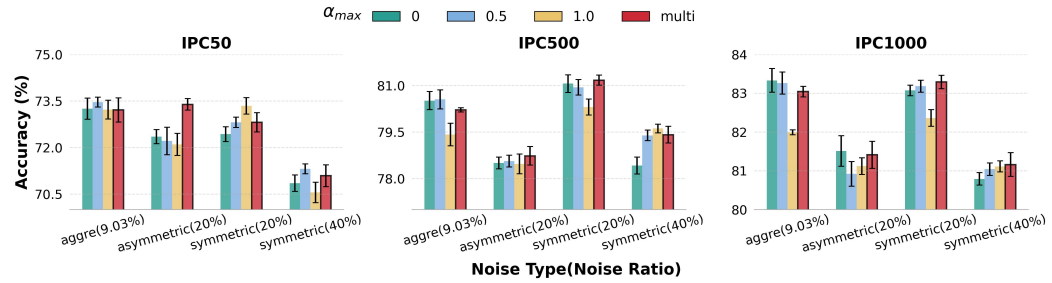
The Impact of Each Component. We conduct an ablation study on the CIFAR-10 dataset under symmetric label noise levels of 20% and 40%, evaluating model performance across varying data condensation settings ($IPC \in 10, 50, 500, 1000$). Starting from the DATM baseline, we progressively incorporate our proposed components: *Selective Guidance Reweighting* (SGR) and *Teacher-Inspired Auxiliary Targets* (TIAT). As shown in Table 2, introducing SGR yields consistent performance gains, particularly under severe noise and limited data (e.g., +4.7% at 10 IPC with 40% noise), demonstrating the effectiveness of trajectory-level denoising. Adding TIAT further improves accuracy, with additional gains such as +5.7% at 500 IPC under 40% noise, highlighting the benefit of leveraging uncertainty-filtered clean supervision. Overall, the combination of SGR and TIAT leads to stable and substantial improvements, validating the robustness and compatibility of our framework in noisy learning environments.

431

Effectiveness of Diverse Sampling To assess the robustness of progressive trajectory diversity, we compare *Diverse Sampling*—where P teacher trajectories are trained with uniformly distributed α_{\max}

432 Table 2: Ablation results on CIFAR-10 under symmetric noise with 20% and 40% corruption ratios, evaluated
 433 across different IPCs (images per class).

Method	IPC	Symmetric (20%)				Symmetric (40%)			
		10	50	500	1000	10	50	500	1000
DATM		62.7	71.7	80.0	81.9	58.2	67.2	74.3	76.7
+ SGR		63.8 (↑1.1)	72.8 (↑1.1)	81.2 (↑1.2)	83.3 (↑1.4)	62.9 (↑4.7)	71.1 (↑3.9)	79.4 (↑5.1)	81.2 (↑4.5)
+ SGR + TIAT		64.5 (↑1.8)	73.5 (↑1.8)	81.5 (↑1.5)	83.3 (↑1.4)	64.8 (↑6.6)	71.6 (↑4.4)	80.0 (↑5.7)	81.4 (↑4.7)



450 Figure 3: Performance comparison between *Diverse Sampling* and *Fixed Sampling* under various settings on
 451 **CIFAR-10**. **Baseline** refers to DATM without our method. **Diverse Sampling** and **Fixed Sampling** incorporate
 452 our **Selective Guidance Reweighting** into DATM, where Fixed Sampling uses fixed α_{\max} values **(0, 0.5, 1.0)** for
 453 teacher trajectory training, while Diverse Sampling **multi** follows the strategy outlined in Section 4.2.

454 values in $[0, 1]$ —against a *Fixed Sampling* baseline with constant α_{\max} . As shown in Figure 3, under
 455 increasing noise levels, the Diverse Sampling strategy consistently outperforms fixed configurations,
 456 exhibiting stable performance without noticeable degradation. In contrast, fixed- α trajectories show
 457 varying sensitivity to the noise rate, indicating their lack of generalizability. These results highlight
 458 that diversity in teacher signal strength improves resilience to label corruption, enabling more robust
 459 and adaptive supervision during distillation.

460 Table 3: Ablation study on the effect of β under symmetric noise (20% and 40%) on CIFAR-10. We
 461 highlight the top two accuracies and the default β .

β	Subset Ratio	Symmetric (20%)			Symmetric (40%)		
		50%	60%	70%	50%	60%	70%
0.1		73.3±0.11	73.5±0.38	73.3±0.4	71.9±0.2	71.5±0.4	71.8±0.1
0.5		72.5±0.29	73.4±0.12	74.0±0.3	71.7±0.3	72.2±0.3	71.4±0.2
1.0		67.4±0.12	69.6±0.17	71.6±0.3	70.0±0.3	71.7±0.2	71.5±0.1

469 **Effect of High-Confidence Subset Proportion and β Coefficient.** We investigate how the clean
 470 subset ratio and the auxiliary loss weight β affect distillation performance under 20% and 40%
 471 symmetric noise on CIFAR-10 (IPC=50). As shown in Table 3, the method is robust across a range of
 472 subset ratios (50%–70%) and β values. While $\beta = 0.5$ yields the highest accuracy in some settings,
 473 $\beta = 0.1$ consistently provides stable performance across noise levels, particularly when combined
 474 with a 60% subset. In contrast, $\beta = 1.0$ tends to degrade performance due to overemphasis on
 475 auxiliary signals. Based on these results, we adopt $\beta = 0.1$ and a 60% subset as default settings for
 476 all main experiments.

478 6 CONCLUSION

480 We investigate the underexplored problem of dataset distillation under noisy-label settings and identify
 481 two key challenges: overfitting to label noise and limited capacity of the synthetic set to retain clean
 482 signals. To address these, we introduce Selective Guidance Reweighting and Teacher-Inspired
 483 Auxiliary Targets. Experiments on benchmark datasets validate the robustness and effectiveness of
 484 our approach, paving the way for future research in noise-resilient dataset distillation.

486 ETHICS STATEMENT
487488 This work does not involve human subjects, animal experiments, or sensitive personal data. The
489 datasets used (e.g., CIFAR-10/100 and their human-annotated variants CIFAR-10N/100N) are publicly
490 available benchmarks commonly used in noisy-label learning research and do not contain personally
491 identifiable information. Our method focuses on improving the robustness of dataset distillation
492 under label noise through trajectory-based reweighting and auxiliary supervision, without introducing
493 harmful, deceptive, or privacy-invasive applications. We have carefully reviewed the ICLR Code of
494 Ethics and confirm that this submission complies with its principles regarding fairness, transparency,
495 and research integrity. The authors declare no conflicts of interest.
496497 REPRODUCIBILITY STATEMENT
498499 To ensure reproducibility, we provide the following: (1) Full implementation details—including
500 network architecture (3-layer ConvNet), distillation pipeline, SGR/TIAT hyperparameters (e.g., α
501 schedule, $\beta=0.1$, 60% high-confidence subset), and noise protocols—are described in Sections 4 and
502 5.1, as well as in Table 3. (2) All experiments are averaged over 5 random seeds, with mean and
503 standard deviation reported. (3) While code is not included due to double-blind review, we commit to
504 releasing anonymized implementation upon acceptance to facilitate replication.
505506 LLM USAGE STATEMENT
507508 Large Language Models (LLMs) were used in this work solely as a general-purpose writing assistance
509 tool—for example, to improve grammar, clarify phrasing, or check technical terminology in the
510 manuscript. LLMs did not contribute to the conception of the research idea (e.g., SGR or TIAT
511 design), theoretical analysis, experimental setup, or interpretation of results. All scientific content,
512 including algorithm design, loss formulations, and empirical claims, was developed and verified by
513 the authors. No LLM was used to generate novel technical content or to draft substantial portions of
514 the paper. As required by ICLR policy, we confirm that LLMs are not listed as authors, and we take
515 full responsibility for all content under our names.
516

517 REFERENCES

518 Dara Bahri, Heinrich Jiang, and Maya Gupta. Deep k-nn for noisy labels. In *International Conference on*
519 *Machine Learning*, pp. 540–550. PMLR, 2020.
520
521 George Cazenavette, Tongzhou Wang, Antonio Torralba, Alexei A. Efros, and Jun-Yan Zhu. Dataset distillation
522 by matching training trajectories, 2022. URL <https://arxiv.org/abs/2203.11932>.
523
524 Xuxi Chen, Yu Yang, Zhangyang Wang, and Baharan Mirzasoleiman. Data distillation can be like vodka:
525 Distilling more times for better quality, 2023. URL <https://arxiv.org/abs/2310.06982>.
526
527 Lechao Cheng, Kaifeng Chen, Jiyang Li, Shengeng Tang, Shufei Zhang, and Meng Wang. Dataset distillers are
528 good label denoisers in the wild. *arXiv preprint arXiv:2411.11924*, 2024.
529
530 Justin Cui, Ruochen Wang, Si Si, and Cho-Jui Hsieh. Dc-bench: Dataset condensation benchmark, 2022. URL
531 <https://arxiv.org/abs/2207.09639>.
532
533 Wenxiao Deng, Wenbin Li, Tianyu Ding, Lei Wang, Hongguang Zhang, Kuihua Huang, Jing Huo, and Yang Gao.
534 Exploiting inter-sample and inter-feature relations in dataset distillation, 2024. URL <https://arxiv.org/abs/2404.00563>.
535
536 Francesco Di Salvo, Sebastian Doerrich, Ines Rieger, and Christian Ledig. An embedding is worth a thousand
537 noisy labels. *arXiv preprint arXiv:2408.14358*, 2024.
538
539 Jiawei Du, Yidi Jiang, Vincent Y. F. Tan, Joey Tianyi Zhou, and Haizhou Li. Minimizing the accumulated
540 trajectory error to improve dataset distillation, 2023. URL <https://arxiv.org/abs/2211.11004>.
541
542 Erik Englesson and Hossein Azizpour. Robust classification via regression for learning with noisy labels. In
543 *ICLR 2024-The Twelfth International Conference on Learning Representations, Messe Wien Exhibition and*
544 *Congress Center, Vienna, Austria, May 7-11t, 2024*, 2024.

540 Ziyao Guo, Kai Wang, George Cazenavette, Hui Li, Kaipeng Zhang, and Yang You. Towards lossless dataset
 541 distillation via difficulty-aligned trajectory matching, 2024. URL <https://arxiv.org/abs/2310.05773>.

543 Bo Han, Quanming Yao, Xingrui Yu, Gang Niu, Miao Xu, Weihua Hu, Ivor Tsang, and Masashi Sugiyama.
 544 Co-teaching: Robust training of deep neural networks with extremely noisy labels. *Advances in neural*
 545 *information processing systems*, 31, 2018.

546 Yang He, Lingao Xiao, Joey Tianyi Zhou, and Ivor Tsang. Multisize dataset condensation, 2024. URL
 547 <https://arxiv.org/abs/2403.06075>.

549 Ahmet Iscen, Jack Valmadre, Anurag Arnab, and Cordelia Schmid. Learning with neighbor consistency for noisy
 550 labels. 2022 ieee. In *CVF Conference on Computer Vision and Pattern Recognition (CVPR)*, pp. 4662–4671,
 551 2022.

552 Lu Jiang, Zhengyuan Zhou, Thomas Leung, Li-Jia Li, and Li Fei-Fei. Mentornet: Learning data-driven
 553 curriculum for very deep neural networks on corrupted labels. In *International conference on machine*
 554 *learning*, pp. 2304–2313. PMLR, 2018.

555 Alex Krizhevsky. Learning multiple layers of features from tiny images, 2009. URL <https://api.semanticscholar.org/CorpusID:18268744>.

556 Yongmin Lee and Hye Won Chung. Selmatch: Effectively scaling up dataset distillation via selection-based
 557 initialization and partial updates by trajectory matching, 2024. URL <https://arxiv.org/abs/2406.18561>.

558 Jichang Li, Guanbin Li, Feng Liu, and Yizhou Yu. Neighborhood collective estimation for noisy label identifica-
 559 tion and correction. In *European Conference on Computer Vision*, pp. 128–145. Springer, 2022.

560 Junnan Li, Richard Socher, and Steven CH Hoi. Dividemix: Learning with noisy labels as semi-supervised
 561 learning. *arXiv preprint arXiv:2002.07394*, 2020.

562 Wen Li, Limin Wang, Wei Li, Eirikur Agustsson, and Luc Van Gool. Webvision database: Visual learning and
 563 understanding from web data, 2017. URL <https://arxiv.org/abs/1708.02862>.

564 Sheng Liu, Jonathan Niles-Weed, Narges Razavian, and Carlos Fernandez-Granda. Early-learning regularization
 565 prevents memorization of noisy labels. *Advances in neural information processing systems*, 33:20331–20342,
 566 2020.

567 Yang Liu and Hongyi Guo. Peer loss functions: Learning from noisy labels without knowing noise rates. In
 568 *International conference on machine learning*, pp. 6226–6236. PMLR, 2020.

569 Noel Loo, Ramin Hasani, Mathias Lechner, and Daniela Rus. Dataset distillation with convexified implicit
 570 gradients, 2023. URL <https://arxiv.org/abs/2302.06755>.

571 Yueming Lyu and Ivor W Tsang. Curriculum loss: Robust learning and generalization against label corruption.
 572 *arXiv preprint arXiv:1905.10045*, 2019.

573 Pratyush Maini, Saurabh Garg, Zachary Lipton, and J Zico Kolter. Characterizing datapoints via second-split
 574 forgetting. *Advances in Neural Information Processing Systems*, 35:30044–30057, 2022.

575 Eran Malach and Shai Shalev-Shwartz. Decoupling" when to update" from" how to update". *Advances in neural*
 576 *information processing systems*, 30, 2017.

577 Timothy Nguyen, Roman Novak, Lechao Xiao, and Jaehoon Lee. Dataset distillation with infinitely wide convo-
 578 lutional networks. *CoRR*, abs/2107.13034, 2021. URL <https://arxiv.org/abs/2107.13034>.

579 Scott Reed, Honglak Lee, Dragomir Anguelov, Christian Szegedy, Dumitru Erhan, and Andrew Rabinovich.
 580 Training deep neural networks on noisy labels with bootstrapping. *arXiv preprint arXiv:1412.6596*, 2014.

581 Noveen Sachdeva and Julian McAuley. Data distillation: A survey, 2023. URL <https://arxiv.org/abs/2301.04272>.

582 Jun Shu, Qi Xie, Lixuan Yi, Qian Zhao, Sanping Zhou, Zongben Xu, and Deyu Meng. Meta-weight-net:
 583 Learning an explicit mapping for sample weighting. *Advances in neural information processing systems*, 32,
 584 2019.

585 Hwanjun Song, Minseok Kim, and Jae-Gil Lee. Selfie: Refurbishing unclean samples for robust deep learning.
 586 In *International conference on machine learning*, pp. 5907–5915. PMLR, 2019.

594 Hwanjun Song, Minseok Kim, Dongmin Park, Yooju Shin, and Jae-Gil Lee. Learning from noisy labels with
 595 deep neural networks: A survey. *IEEE transactions on neural networks and learning systems*, 34(11):
 596 8135–8153, 2022.

597 Yuanpeng Tu, Boshen Zhang, Yuxi Li, Liang Liu, Jian Li, Yabiao Wang, Chengjie Wang, and Cai Rong Zhao.
 598 Learning from noisy labels with decoupled meta label purifier. In *Proceedings of the IEEE/CVF Conference
 599 on Computer Vision and Pattern Recognition*, pp. 19934–19943, 2023.

600 Shaobo Wang, Yicun Yang, Zhiyuan Liu, Chenghao Sun, Xuming Hu, Conghui He, and Linfeng Zhang. Dataset
 601 distillation with neural characteristic function: A minmax perspective, 2025. URL <https://arxiv.org/abs/2502.20653>.

602 Tiansheng Wang, Jun Huan, and Bo Li. Data dropout: Optimizing training data for convolutional neural networks.
 603 In *2018 IEEE 30th international conference on tools with artificial intelligence (ICTAI)*, pp. 39–46. IEEE,
 604 2018a.

605 Tongzhou Wang, Jun-Yan Zhu, Antonio Torralba, and Alexei A. Efros. Dataset distillation. *CoRR*,
 606 [abs/1811.10959](https://arxiv.org/abs/1811.10959), 2018b. URL [http://arxiv.org/abs/1811.10959](https://arxiv.org/abs/1811.10959).

607 Jiaheng Wei, Zhaowei Zhu, Hao Cheng, Tongliang Liu, Gang Niu, and Yang Liu. Learning with noisy labels
 608 revisited: A study using real-world human annotations. *arXiv preprint arXiv:2110.12088*, 2021.

609 Hansong Zhang, Shikun Li, Fanzhao Lin, Weiping Wang, Zhenxing Qian, and Shiming Ge. Dance: Dual-
 610 view distribution alignment for dataset condensation, 2024a. URL <https://arxiv.org/abs/2406.01063>.

611 Hansong Zhang, Shikun Li, Pengju Wang, Dan Zeng, and Shiming Ge. M3d: Dataset condensation by
 612 minimizing maximum mean discrepancy, 2024b. URL <https://arxiv.org/abs/2312.15927>.

613 Zhilu Zhang and Mert Sabuncu. Generalized cross entropy loss for training deep neural networks with noisy
 614 labels. *Advances in neural information processing systems*, 31, 2018.

615 Bo Zhao and Hakan Bilen. Dataset condensation with distribution matching, 2022. URL <https://arxiv.org/abs/2110.04181>.

616 Bo Zhao, Konda Reddy Mopuri, and Hakan Bilen. Dataset condensation with gradient matching, 2021. URL
 617 <https://arxiv.org/abs/2006.05929>.

618 Tianyi Zhou, Shengjie Wang, and Jeff Bilmes. Robust curriculum learning: from clean label detection to noisy
 619 label self-correction. In *International Conference on Learning Representations*, 2021.

620 Yongchao Zhou, Ehsan Nezhadarya, and Jimmy Ba. Dataset distillation using neural feature regression, 2022.
 621 URL <https://arxiv.org/abs/2206.00719>.

622 Yuyin Zhou, Xianhang Li, Fengze Liu, Qingyue Wei, Xuxi Chen, Lequan Yu, Cihang Xie, Matthew P Lungren,
 623 and Lei Xing. L2b: Learning to bootstrap robust models for combating label noise. In *Proceedings of the
 624 IEEE/CVF Conference on Computer Vision and Pattern Recognition*, pp. 23523–23533, 2024.

625 Zhaowei Zhu, Zihao Dong, and Yang Liu. Detecting corrupted labels without training a model to predict. In
 626 *International conference on machine learning*, pp. 27412–27427. PMLR, 2022.

627
 628
 629
 630
 631
 632
 633
 634
 635
 636
 637
 638
 639
 640
 641
 642
 643
 644
 645
 646
 647